Plant Physiol. (1990) 93, 471–478
0032-0889/90/93/0471/08/$01.00/0

Received for publication September 18, 1989
and in revised form January 6, 1990

Electrostatic Changes in *Lycopersicon esculentum* Root Plasma Membrane Resulting from Salt Stress

Charles G. Suhayda, John L. Giannini, Donald P. Briskin, and Michael C. Shannon*

Department of Crop Science and Plant Ecology, University of Saskatchewan, Saskatoon, Saskatchewan S7N OWO Canada (C.G.S.); Biology Department, St. Olaf College, Northfield, Minnesota 55057 (J.L.G.); Department of Agronomy, University of Illinois, Urbana, Illinois 61801 (D.P.B.); and U.S. Department of Agriculture-Agricultural Research Service, U.S. Salinity Laboratory, Riverside, California 92501 (M.C.S.)

ABSTRACT

Salinity-induced alterations in tomato (*Lypersicon esculentum* Mill. cv Heinz 1350) root plasma membrane properties were studied and characterized using a membrane vesicle system. Equivalent rates of MgATP-dependent H^+-transport activity were measured by quinacrine fluorescence (ΔpH) in plasma membrane vesicles isolated from control or salt-stressed (75 millimolar salt) tomato roots. However, when bis-[3-phenyl-5-oxoisoxazol-4-yl] pentamethine was used to measure MgATP-dependent membrane potential ($\Delta\psi$) formation, salt-stressed vesicles displayed a 50% greater initial quench rate and a 30% greater steady state quench than control vesicles. This differential probe response suggested a difference in surface properties between control and salt-stressed membranes. Fluorescence titration of vesicles with the surface potential probe, 8-anilino-1-napthalenesulphonic acid (ANS) provided dissociation constants (K_d) of 120 and 76 micromolar for dye binding to control and salt-stressed vesicles, respectively. Membrane surface potentials (ψ_o) of −26.0 and −13.7 millivolts were calculated for control and salt-stressed membrane vesicles from the measured K_d values and the calculated intrinsic affinity constant, K_i. The concentration of cations and anions at the surface of control and salt-stressed membranes was estimated using ψ_o values and the Boltzmann equation. The observed difference in membrane surface electrostatic properties was consistent with the measured differences in K^+-stimulated kinetics of ATPase activity between control and salt-stressed vesicles and by the differential ability of Cl^- ions to stimulate H^+-transport activity. Salinity-induced changes in plasma membrane electrostatic properties may influence ion transport across the plasma membrane.

The plasma membrane is an important interface between the apoplastic space and the cytoplasm. The MgATP-dependent proton pumping ATPase associated with this membrane generates and maintains an electrochemical gradient resulting in an acid exterior ΔpH[1] and an interior negative membrane $\Delta\psi$ (26).

Essential ions and solutes can thus be co- or countertransported by membrane-bound carriers at the expense of the electrochemical gradient (15). The biochemical properties (18) and the proton pump activity (26) of the plasma membrane-bound, ion-stimulated ATPase have been reported for a variety of plant species. These studies have focused mainly on the characterization of ATPase and proton pump activities on membrane fractions isolated from nonstressed tissues. The relationship between proton pump activity and cellular ion regulation is especially important in salt-stressed tissues. With this thought, we focused our investigation on salt-induced changes in plasma membrane function.

Giannini *et al.* (10) describe a method for the isolation of plasma membrane-enriched vesicles that are transport competent and retain full activity for a prolonged time period when stored at −80°C. Using this plasma membrane vesicle system, we initiated a comparative study of proton transport, and membrane-bound ATPase activity in native vesicles isolated from control and salt-stressed tomato roots (*Lycopersicon esculentum* Mill. cv Heinz 1350). Characterization of salt stress effects on proton pump activity, ATPase kinetics, and the ion-stimulation of these processes provides essential information that is necessary to understand the role of the plasma membrane in the physiological mechanisms of salt tolerance.

MATERIALS AND METHODS

Plant Material

Tomato (*Lypersicon esculentum* Mill. cv Heinz 1350) seeds were germinated in vermiculite for 1 week and then were placed into aerated hydroponic solution culture (0.5× Hoagland solution [pH 6.0]) and maintained in a growth chamber. The plants were provided with 16 h daylight at a light intensity of 250 $\mu E\ m^{-2}\ s^{-1}$. Day/night temperatures were maintained at 30°C/25°C. Salt stress was applied 10 d after transplanting at a rate of 0.1 MPa d^{-1} (15 mM NaCl, 3 mM $CaCl_2$) for 4 consecutive days resulting in a 75 mM applied salt stress at a Na:Ca ratio of 5:1. The plants were 35-d-old at harvest.

Plasma Membrane Isolation

The plasma membrane-enriched vesicle fractions that were used for ion transport measurements were isolated by the method of Giannini *et al.* (10); all solutions were kept at ice

[1] Abbreviations: ΔpH, pH gradient; $\Delta\psi$, electrical potential difference; ANS, 8-anilino-1-naphthalenesulfonic acid; BTP, bis-tris propane; Oxonol V, bis-[3-phenyl-5-oxoisoxazol-4-yl]pentamethine; Ψ_o, surface potential.

water temperature, and all procedures were performed on ice. Excised tomato roots were briefly rinsed with deionized water, blotted to remove excess water, cut into small segments, and immediately placed into the homogenizing buffer. This buffer consisted of 70 mM Tris-HCl (pH 8.0) with 250 mM sucrose and contained the following: 10% (v/v) glycerol, 3 mM EDTA, 2 mM PMSF, 4 mM DTE, 15 mM β-mercaptoethanol, 2 mM Na_2ATP, and 250 mM KI. Prior to hand homogenization by mortar and pestle the root tissue was vacuum infiltrated for 5 min with homogenizing buffer. The homogenate was filtered through four layers of cheesecloth and then centrifuged for 15 min at 13,000*g* using a Sorvall[2] SS34 rotor. The resulting supernatant was centrifuged at 85,000*g* using a Beckman 45 Ti rotor for 30 min. The supernatant was discarded and the microsomal pellet was carefully suspended and gently homogenized with a ground glass homogenizer in a buffer consisting of 2 mM BTP-Mes (pH 7.0) with 250 mM sucrose and containing the following: 10% (v/v) glycerol, 1 mM DTE, 1 mM PMSF. Sucrose solutions for the density gradients were prepared in 1 mM BTP-Mes (pH 7.0) and contained 1 mM DTE. In initial studies, the buoyant densities of various membrane components were determined by layering the resuspended microsomes on a 36-mL linear 15 to 45% (w/w) continuous sucrose gradient. The gradient was centrifuged at 100,000*g* for 4 h in a Beckman SW 28 rotor and fractionated into 1.5 mL aliquots. For routine preparation of plasma membrane-enriched fractions, microsomes were layered onto a discontinuous sucrose gradient (34/40%) and centrifuged in a Beckman SW 28 rotor at 100,000*g* for 2 h. The plasma membrane fraction was recovered at the sucrose gradient interface and the samples were either used immediately or stored in liquid N_2. Full transport activity was maintained for at least 1 month under these conditions.

Measurement of ΔpH, Δψ, and ATPase Activity

Proton transport activity was monitored by the measurement of ΔpH and Δψ in the plasma membrane vesicles upon addition of MgATP. The quenching of the fluorescent probes, quinacrine (pH-sensitive) or Oxonol V (potential-sensitive) was used to measure ΔpH or Δψ, respectively. Fluorescence measurements were recorded with a SPEX model 112A fluorimeter at 25°C. Excitation and emission wavelengths for quinacrine were 430 and 500 nm, respectively; and 580 and 650 nm for Oxonol V, respectively. Excitation and emission slit widths were 1.25 mm. The vesicles were assayed by placing 50 μg membrane protein into a buffered solution consisting of 25 mM BTP-Mes (pH 7.0) with 250 mM sorbitol and containing the following: 3.75 mM $MgSO_4$, 3.75 mM ATP (BTP salt), and 50 mM monovalent ions (when present). For all assays, quinacrine (ΔpH) was present at a final concentration of 2.5 μM Oxonol V (Δψ) was present at a final concentration of 0.5 μM. Fluorescence quenching assays were quantitated by determining the initial rate of quench (%Q/min/mg), or by the ionophore reversible quench at the steady state (%Q/mg) determined after the addition of 5 μM gramicidin (2).

ATPase assays were performed in 25 mM BTP-Mes (pH 7.0) buffer containing 3.75 mM $MgSO_4$, 3.75 mM ATP (BTP salt), and 5 μM gramicidin. Monovalent ions and specific ATPase inhibitors were added as required. Plasma membrane-bound ATPase activity was determined by the difference in activity between assays supplemented with 50 mM KCl or 50 mM KCl plus 100 μM sodium orthovanadate (24). Mitochondrial ATPase activity was determined from the difference in activity observed with 50 mM KCl or 50 mM KCl plus 1 mM NaN_3 (24). Tonoplast activity was determined from the difference in activity measured in assays containing 50 mM KCl and those with 50 mM KNO_3 (24). Latent UDPase, a marker for Golgi membrane, was assayed as described by Nagahashi and Nagahashi (21).

Measurement of Surface Potential

Plasma membrane vesicles were titrated with the anionic, fluorescent probe ANS obtained from Kodak. Surface potentials were estimated by the method of Gibrat *et al.* (11). Excitation and emission wavelengths for the dye were 360 and 480 nm, respectively, and cutoff filters were used to minimize scattered light. Titrations with ANS were made in a buffered system (25 mM BTP-Mes [pH 7.0], 0.25 M sorbitol) by successive additions of dye (5–5000 μM) to the stirred vesicle suspension (75 μg protein/3 mL). Following a 1-min dye equilibration period, data were collected by signal averaging for 2 min. To preclude inner filter effects, the optical density of the dye plus sample was maintained at less than 0.05 (17).

Protein and Pi Determination

The colorimetric assay of Peterson (22) was used to determine membrane protein concentration using BSA as the protein standard. Inorganic phosphate was measured by the colorimetric method of Peterson (23).

RESULTS

Membrane Characterization

Microsomal membrane fractions obtained by differential centrifugation from control and salt-stressed tomato roots were separated on sucrose gradients. Inhibitor-sensitive ATPase activities were used to map the distribution of membrane-associated marker enzymes in 15 to 45% linear gradients (Fig. 1). Analysis of microsomes from control roots (Fig. 1A) localized the orthovanadate-sensitive, K^+-stimulated, Mg-ATPase activity peak at 36 to 38% sucrose, which corresponds to a density of 1.16 to 1.17 g cm^{-3} and is associated with plasma membrane (6, 26). This activity overlapped with vanadate-sensitive, MgATP-dependent H^+-pump activity. Latent UDPase activity, a biochemical marker for Golgi membrane (21), was maximum in the 30 to 33% sucrose region of the gradient at a density of 1.13 to 1.14 g cm^{-3} (data not shown). Because of the close proximity of the Golgi membrane density to that of the plasma membrane, we cannot preclude the presence of some Golgi membrane in the plasma

[2] Mention of a trademark, vendor, or proprietary product does not constitute a guarantee or warranty of the product by the U.S. Department of Agriculture and does not imply its approval to the exclusion of other products or vendors that may also be suitable.

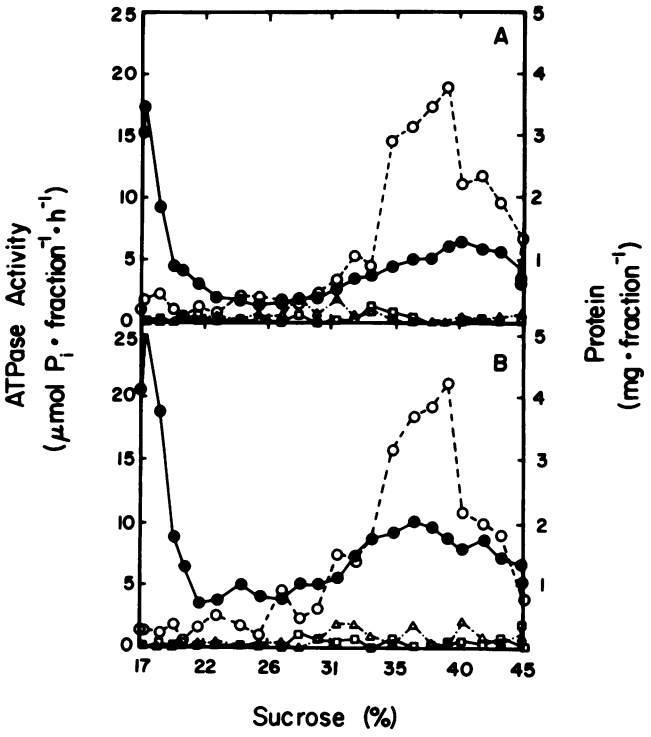

Figure 1. Distribution of vanadate (○), nitrate (△), and azide-sensitive (□) ATPase activity relative to protein concentration (●) in fractions from sucrose gradients of control (A) and salt-stressed (B) tomato root membranes. Assay mixture for ATPase activity contained 25 mM BTP-Mes (pH 7.0), 3.75 mM $MgSO_4$, 3.75 mM ATP (BTP salt), 50 mM KCl and, when present, one of the following inhibitors: 100 μM sodium orthovanadate or 1 mM NaN_3. Tonoplast ATPase activity was determined by substituting 50 mM KNO_3 for KCl in the mixture.

membrane-enriched fractions collected from sucrose step gradients. In a previous report, we examined the latent UDPase activity of the 34/45% interfaces of a sucrose gradient layered with tomato root microsomes (14). The data showed that over 80% of the Golgi-associated latent UDPase activity remained at the overlay/34% sucrose interface. This suggests that Golgi membranes have a slightly lower density than plasma membrane fractions routinely prepared on discontinuous sucrose gradients isolated from the 34/40% sucrose interface. Proton transport associated with these vesicles displayed vanadate sensitivity and NO_3^- and azide insensitivity (Table I). The distribution of the vanadate-sensitive membrane fraction within the sucrose gradient was not altered when microsomes obtained from salt-stressed roots were separated (Fig. 1B). The sucrose gradient characterization of tomato root membrane fractions showed that the application of a 75 mM salt stress did not alter the apparent density of root cell plasma membranes, as determined under the condition of this isolation protocol. Although differences in plasma membrane density were not observed, this does not preclude possible variations in membrane proteins and lipids on the microscopic level as a result of salt stress.

MgATPase Activity and K^+-Stimulated ATPase Kinetics in Control and Salt-Stressed Plasma Membranes

The basal MgATPase activity of control and salt-stressed plasma membrane fractions measured at a MgATP concentration of 3.0 mM in the absence of monovalent ions did not differ in having values of 23.1 and 22.4 μmol Pi (mg protein)$^{-1}$ h^{-1}, respectively. Differences between control and salt-stressed membrane fractions were readily evident when the K^+-stimulation of basal MgATPase activity was measured (Fig. 2). Membranes isolated from control, 50 mM, and 75 mM salt-stressed tomato roots showed reductions in K^+-stimulated ATPase activity that were in proportion to the applied stress. A kinetic analysis showed that the apparent K_m for K^+ remained relatively constant, whereas the V_{max} for K^+-stimulation was reduced by 22 and 39% in membranes isolated from 50 and 75 mM salt-stressed roots, respectively (see Fig. 2 legend).

ΔpH and Δψ Development in Control and Salt-Stressed Plasma Membrane Vesicles

MgATP-dependent H^+-transport activity in tomato root plasma membrane vesicles displayed a broad pH dependence with peak activity near pH 7.5 (Fig. 3). This pH regulation of proton pump activity has also been demonstrated for corn root plasma membranes (25). In the corn membrane system the decrease in H^+-pump activity associated with a change in pH from 7.0 to 5.5 was correlated with a decrease in membrane microviscosity. To avoid the imposition of a pH gradient across the membrane prior to the start of transport assays, the vesicle suspensions (isolated in pH 7.0 buffer) were routinely assayed at pH 7.0. The MgATP-dependent proton pump activity measured at pH 7.0 with control membrane vesicles and determined in the presence of 50 mM KCl displayed saturation kinetics with increasing concentrations of MgATP (Fig. 4). The kinetic parameters determined by means of the Hanes-Woolf plot (Fig. 4, inset) were V_{max} = 67% Q/mg/min and K_m = 0.06 mM for MgATP (5).

The comparative ability of control and salt-stressed plasma membrane vesicles to generate pH and membrane potential gradients is shown in Figure 5. The MgATP-dependent formation of pH gradients measured in control and stressed membrane vesicles using the quinacrine quench assay showed that salt stress did not influence ΔpH formation (Fig. 5A). The MgATP-dependent, curvilinear quenching of quinacrine fluorescence by a membrane vesicle suspension most likely represents a two-component system consisting of initial quench rate and the steady state quench (1, 9). The initial rate of dye quenching reflects the initial rate of proton pumping and is proportional to the rate of MgATP hydrolysis. The steady state quench may reflect an equilibrium condition where the rate of protons accumulated in the vesicle is equivalent to the rate of H^+ efflux from the vesicle interior. It is apparent from the quinacrine quench curves that salt stress did not alter either the initial quench rate or the percent quench (%Q) measured at 5 min, which was near the steady state, during ΔpH formation (Fig. 5A; Table I).

Proton pumping, as measured by quinacrine fluorescence, is ion stimulated (Table I). In control and salt-stressed vesicles the enhancement of fluorescence is in the order: KNO_3>KCl>NaCl (KNO_3 was not tested in salt-stressed vesicles). The effectiveness of these salts in the dissipation of membrane potential followed the same sequence: KNO_3>KCl>NaCl (Table I). Rapid entry of the permeant anions NO_3^- and Cl^- into the vesicle interior results in the

Table I. *Measurement of ΔpH and Δψ in Control and Salt-Stressed Plasma Membrane Vesicles—MgATP Dependence and Ion Effects*

Treatment	Experiment 1		Experiment 2	
	Control	Stressed	Control	Stressed
		ΔpH (%Q/mg)		
MgATP (3.75 mM)	92 (3)[a]	91 (2)	102 (2)	111 (8)
MgATP + 50 mM KCl	200	216	218	
MgATP + 50 mM NaCl	168	151	177	
MgATP + 50 mM KNO_3	276		263	
MgATP + 50 mM KCl + 100 μM Na_3VO_4			148	
MgATP + 50 mM KCl + 1 mM NaN_3			218	
		ΔΨ (%Q/mg)		
3.75 mM MgATP	342 (20)	447 (34)	366 (26)	511 (33)
3.75 + 50 mM KCl	169		241	377
3.75 + 50 mM NaCl	184		255	413
3.75 + 50 mM KNO_3	65		108	126

[a] Numbers in parentheses represent standard deviations based on three measurements.

collapse of the potential gradient due to charge compensation and stimulates pump activity. The stimulation of ΔpH by monovalent cation likely results from direct stimulation of the ATPase. Similar results have been reported in red beet (9).

The ability of Cl^- to stimulate H^+-pumping and enhance ΔpH in control and salt-stressed vesicles is shown in Table II. The addition of increasing concentrations of Cl^--BTP stimulate ΔpH above the level of MgATP for both control and stressed vesicles. However Cl^- stimulation of ΔpH in salt-stressed vesicles was about 2-fold greater at 25 and 50 mM added Cl^- and 1.25-fold greater at 100 mM added Cl^- than for control vesicles. When the MgATP-dependent, Δψ formation was measured using the anionic, potential-sensitive dye Oxonol V, a striking difference between control and saltstressed vesicles was observed (Fig. 5B). Salt-stressed vesicles had an initial quench rate of 357% Q/min/mg (measured at 60 s). This was approximately 50% greater than the initial quench rate in control vesicles (242% Q/min/mg). A difference in the steady state quench (measured at 5 min) was also evident with salt-stressed vesicles developing consistently greater potential gradients (on the average 30% larger) than control vesicles (Table I).

Thus, measurement of ΔpH and Δψ in control and salt-stressed plasma membrane vesicles yielded contradictory re-

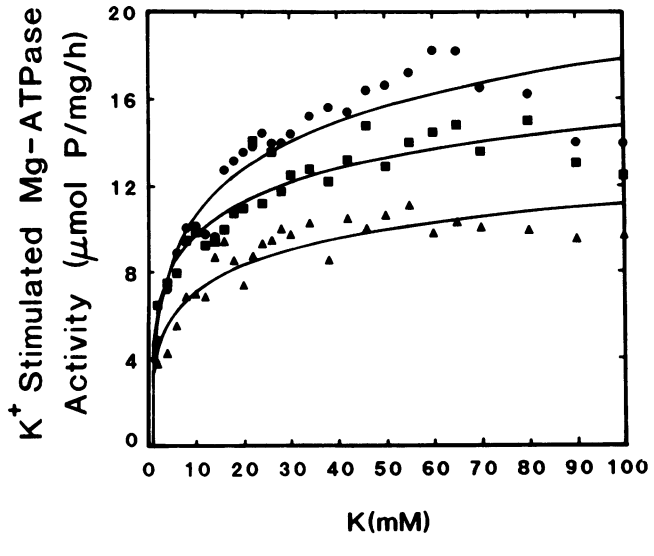

Figure 2. K^+-stimulated MgATPase activity of tomato root plasma membrane vesicles isolated from plants grown in control (●), 50 mM salt (■), and 75 mM salt (▲) solutions. The kinetic parameters were: V_{max} = 18.8, 14.7, and 11.5 μmol Pi (mg protein)$^{-1}$ h^{-1}; and values for K_m = 6.7, 5.3, and 6.0 mM for the respective treatments.

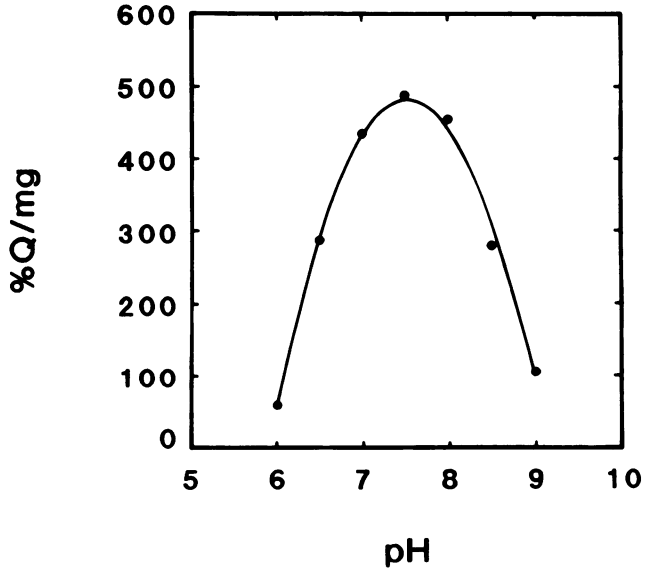

Figure 3. MgATP-dependent H^+-transport activity of tomato plasma membrane vesicles as a function of pH. Ionophore-reversible quench activity was determined in a 2.2 mL assay mixture containing 25 mM BTP-Mes (pH 7.0), 250 mM sorbitol, 3.75 mM $MgSO_4$, 3.75 mM ATP (BTP salt), 2.5 μM quinacrine, and 50 μg membrane protein.

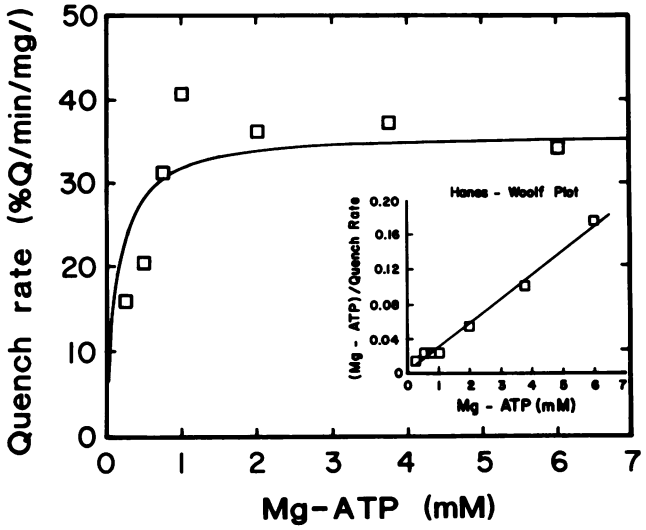

Figure 4. MgATP-dependence and saturation kinetics of proton pump activity at pH 7.0 of control membrane vesicles as determined in the presence of 50 mM KCl and increasing concentrations of MgATP. Quench rates were determined in a 2.2 mL assay mixture containing 25 mM BTP/Mes (pH 7.0), 250 mM sorbitol, 3.75 mM ATP (BTP salt), 2.5 μM quinacrine, 50 μg membrane protein, and $MgSO_4$ as indicated. The kinetic parameters as determined by means of the Hanes-Woolf plot (inset) were V_{max} = 67% Q/mg/min and K_m = 0.06 mM for MgATP.

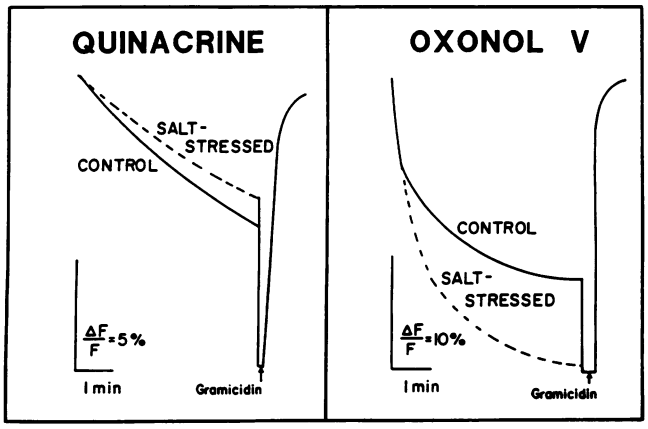

Figure 5. Comparison of the abilities of control and salt-stressed plasma membrane vesicles to generate pH (quinacrine response) or membrane potential (Oxonol V response) gradients. The 2.2 mL assay mixture contained 25 mM BTP-Mes (pH 7.0), 250 mM sorbitol, 3.75 mM $MgSO_4$, 3.75 mM ATP (BTP salt), 50 μg membrane protein and either 2.5 μM quinacrine or 0.5 μM Oxonol V.

sults. Using MgATP as the only substrate and in the absence of all other ions, the quench data provided by quinacrine and Oxonol V fluorescence should be in agreement because both probes measure the accumulation of protons within the inverted plasma membrane vesicles. It may be noted however, that the mechanisms by which the probes report proton accumulation differs. The pH sensitive probe, quinacrine, initially exists in equilibrium between its protonated and

Table II. *Effect of Cl^- Ion upon ΔpH in Control and Salt-Stressed Plasma Membrane Vesicles*

Treatment	Control		Stressed	
	%Q/mg	Cl^- stimulation	%Q/mg	Cl^- stimulation
MgATP (3.75 mM)	92 (3)[a]		91 (2)	
MgATP + 25 mM Cl	106 (3)	14	121 (10)	30
MgATP + 50 mM Cl	123 (6)	31	151 (7)	60
MgATP + 100 mM Cl	148 (10)	56	161 (13)	70

[a] Numbers in parentheses represent standard deviations based on three measurements.

zwitterionic forms in both the bulk solution and in the solution encapsulated by the vesicle. When MgATP is added, protons are pumped into the vesicle interior resulting in increased proton concentration as well as an increased quantity of positive charge within the vesicle. The zwitterionic quinacrine molecules within the vesicle are protonated and trapped, resulting in a shift in equilibrium between the zwitterionic quinacrine molecules distributed across thee vesicle membrane. In response, there is a net influx of the quinacrine zwitterion into the vesicle. Oxonol V is an anionic, charge-sensitive probe. It partitions into the vesicle interior in response to the increase in positive charge caused by proton accumulation.

To explain the observed differences in the response of the two probes, we proposed that the differences in fluorescence of the Oxonol V dye might reflect differences in the membrane microenvironment through which this voltage-sensitive anion must pass as it partitions into the vesicle. The increased quenching of Oxonol V in salt-stressed vesicles compared to control vesicles indicated that salt stress may alter the surface charge of plasma membrane vesicles; thus making the membrane more permeable to the dye.

Salt Stress Effects on Membrane Surface Potential

In order to investigate this possibility, we used the anionic, fluorescent dye ANS to measure membrane surface potential. ANS has been used to effectively estimate the microscopic surface potential (Ψ_o) of both plant and mammalian membranes (3, 11, 12). Dye binding to the membrane results in the enhancement of ANS fluorescence and the rapid partitioning ($t_{1/2}$ about 8 s) of the dye between the outer and inner membrane surface (3).

Titration of control and salt-stressed plasma membrane vesicles in the presence of 0, 0.05, and 1.5 M KCl resulted in fluorescence curves displaying saturation kinetics from which the dissociation constant (K_d) were determined (Table III). Determination of K_d under two salt concentrations allowed for the calculation of an intrinsic binding constant (K_i) using the equation (11):

$$K_i = \frac{(K_d)_1 \sqrt{r[(K_d)_2/(K_d)_1]} - (K_d)_2}{\sqrt{r[(K_d)_2/(K_d)_1]} - 1} \quad (1)$$

where $r = \epsilon_1 \cdot [KCl]_1/\epsilon_2 \cdot [KCl]_2$ and ϵ_1 and ϵ_2 are the dielectric constants of the salt solutions. In this case K_i represents the dye binding constant under conditions where Ψ_o is zero.

Table III. *Apparent and Intrinsic Dissociation Constants for ANS Binding and Estimated Surface Potentials for Control and Salt-Stressed Plasma Membranes*

KCl	Apparent Dissociation Constant, K_d		Surface Potential, Ψ_0	
	Control	Stressed	Control	Stressed
M	*μM*		*mV*	
0	120	76	−26.0	−13.7
0.05	103	78	−22.1	−14.4
1.5	52	50	−4.5	−2.9

Intrinsic Dissociation Constant, K_i	
Control	Stressed
μM.	
43	45

Determination of K_d and K_i allowed us to calculate Ψ_0 from (11):

$$\Psi_0 = (kT/e) \ln K_i/K_d \quad (2)$$

where k is the Boltzmann constant, and e is the electronic charge. In all equations R and T stand for the universal gas constant and temperature, respectively. As shown in Table III, salt stress profoundly influenced membrane surface potential reducing it by 47% to a value of −13.7 mV as compared to −26.0 mV for control membranes. The ability of monovalent ions to screen charges on the membrane surface and thus reduce Ψ_0 is also evident as Ψ_0 is greatly suppressed by 1.5 M KCl (Table III).

Additionally, the Ψ_0 values for control and salt-stressed membranes can be used to estimate the concentration of ions at the membrane surface from the Boltzmann equation (16):

$$C_{surface} = C_{bulk} \exp(-ZF\Psi_0/RT) \quad (3)$$

where Z is the valency of the ion, F is the Faraday constant, C_{bulk} is the bulk ion concentration. Table IV shows the estimated cation and anion concentrations at the membrane surface based on Ψ_0 for control and salt-stressed plasma membrane vesicles, and calculated using a solution concentration of 50 mM for monovalent cations and anions and a 5 mM divalent cation concentration. In comparison to control membranes, the concentration of monovalent and divalent cations at the surface of salt-stressed membranes is reduced by 38 and 62%, respectively, whereas monovalent anion concentrations increased by 61% (Table IV).

Table IV. *Surface Potential-Dependent Ion Concentrations ($C_{surface}$) at the Surface of Control and Salt-Stressed Plasma Membranes*

Treatment	Surface Potential	Monovalent Ions[a]		Divalent Ions[b]
		Cations	Anions	Cations
	mV	*mU*		*mM*
Control	−26.0	137.6	18.2	37.8
Stressed	−13.7	85.2	29.3	14.5

[a] Calculated for bulk ion concentration of 50 mM using Equation 3.
[b] Calculated for a bulk ion concentration of 5 mM using Equation 3.

DISCUSSION

The root cell plasma membrane is an important control point for the exclusion or selective uptake of essential ions into the cell using the electrochemical gradient generated by the proton pump. With this in mind, we examined the effects of excess salts in the growth medium on the activity of the plasma membrane-bound proton pumping ATPase isolated from tomato roots. Our results indicate that salt stress does not directly affect MgATP-dependent proton pumping or ATPase activity (Table I; Fig. 5) as measured by quinacrine quenching or ATPase assay. This finding suggests that the number of enzyme molecules in the membrane is not altered by salinity stress. A recent study of yeast plasma membrane ATPase activity during the growth cycle of this organism revealed that as enzyme activity peaked then declined, the levels of antibody detectable ATPase and ATPase mRNA remained relatively constant during this same cycle (8). These authors, using plasma-mediated gene dosage experiments, also showed that overproduction of ATPase reduced cell growth. They concluded that modulation of ion transport at the plasma membrane of yeast occurred by a mechanism that did not involve changing the number of ATPase molecules in the membrane.

Previous work indicates that the interaction of ions with membranes is strongly influenced by the electrostatic properties of the membrane (16). Our data demonstrate that the root cell modulates the electrostatic properties of the plasma membrane in response to high external salt levels. This is clearly shown by direct measurement of the average membrane surface potential (*i.e.* average of the inside and outside faces of the membrane) using the fluorescent probe, ANS (Table III). The values we obtained for surface potential in control and salt-stressed membranes were −26.0 and −13.7 mV, respectively, and represents a 48% change toward a more positive surface potential. This electrostatic property has been shown to fall within the range of −8 to −30 mV in other biological membranes (16). More specifically, measurement of the surface potential in corn root plasma membrane using ANS titration yielded a value of −20.0 mV (12), whereas in sarcoplasmic reticulum using stopped-flow kinetic analysis, values of −10 and −15 mV were determined for the outside and inside faces of the membrane, respectively (3).

The membrane surface potential is a function of the membrane surface charge density and the ion concentration in the surrounding solution. In the context of the Gouy-Chapman theory of the diffuse electrical double layer, the magnitude of the surface potential decays with distance from the membrane surface. Its value can be characterized by the Debye length, the distance where the potential reaches $1/e$ of its original value (20). As the ion concentration in the bulk solution increases the Debye length decreases. The plant cell when exposed to a saline environment may compensate for the ion-induced suppression of surface potential with changes in the plasma membrane surface charge density. This change would directly affect membrane surface potential and provide a mechanism by which the cell could (a) maintain a required distance between the ions concentrated near the membrane and the membrane surface itself, and (b) modulate the com-

position of ions in solution (cation:anion ratio) at the membrane surface.

The consequences of a large positive shift in plasma membrane surface potential are apparent in the approximation of ion concentrations at the membrane surface, the cation stimulation of ATPase activity, and anion stimulation of proton transport activity. Using the Boltzmann equation, the concentrations of ions at the membrane surface can be estimated if the bulk ion concentration and membrane surface potential are known (16). Application of this procedure to the tomato membrane system predicts a 40% and 62% decrease in the surface concentrations of monovalent and divalent cations, respectively, whereas, monovalent anion concentrations increase by 60% (Table IV). The predicted ion interactions with the plasma membrane are reflected in the K^+-stimulation of MgATPase activity (Fig. 2). The kinetic analysis clearly shows a salt stress-dependent reduction in the apparent V_{max} of K^+-stimulation. A comparison of V_{max} values for control and 75 mM salt-stressed membranes shows a 40% reduction from 18.8 to 11.5 μmol Pi (mg protein)$^{-1}$ h^{-1}, respectively. Similarly, Cl^--stimulation of proton pumping was approximately twofold greater in salt-stressed plasma membrane vesicles than in control vesicles as measured by quinacrine quenching (Table II).

The modulation of the plasma membrane surface potential by the cell to a more positive value could have distinct advantage with respect to salt tolerance. A more positive membrane surface would serve to attract more anions, thus increasing their likelihood of transport into the cell where they could be useful in osmotic adjustment and charge compensation. The attraction of monovalent cations to the membrane surface would diminish as would, presumably, their likelihood of transport. More important though, the monovalent cation stimulation of ATPase is decreased. The modulation of the electrostatic properties of the plasma membrane may represent a mechanism by which the cell limits the stimulation of ATPase activity by monovalent cations when potentially high concentrations of these ions have accumulated intracellularly during salt stress. One disadvantage to a more positive surface potential is the predicted decrease in calcium ions at the membrane surface by the Boltzmann equation. Calcium binding to biomembranes has been shown to be influenced by the percent composition of negatively charged lipid species in a phosphatidylserine/phosphatidylcholine liposome system (7). A decrease in phosphatidylserine content of the liposome resulted in a decline in the calcium that was tightly bound to the membrane and also a decline in the total calcium that was in excess near the membrane surface (4). A decrease in membrane-bound calcium may adversely affect plants in a saline environment where regulation of membrane permeability is essential. Adequate calcium levels supplied to the nutrient solutions of hydroponically grown plants have been shown to influence the tissue ion composition of salt-stressed plants. Leaf tissue analysis of rice and corn varieties salinized iso-osmotically with varying Na^+/Ca^{2+} ratios have shown that as this ratio is decreased, the Na^+ content of the leaf also decreases, whereas, the Ca^{2+} content increases (13, 19).

Clearly, more information is needed with respect to the effects of salt stress on membrane properties if we are to gain a better understanding of how salinity affects the ion permeability of plant membranes. Additional studies are currently in progress to reconcile qualitative differences in plasma membrane properties that are observed when membranes are isolated under varying ionic strength conditions using sucrose gradients or the two phase partition system.

ACKNOWLEDGMENTS

We thank Dr. E. A. Nothnagel for the use of his spectrofluorometer and laboratory and for his suggestions on our work and manuscript. We also thank J. H. Draper for his technical assistance with the membrane isolation and plant growth procedures.

LITERATURE CITED

1. **Bennett AB, Spanswick RM** (1983) Optical measurements of ΔpH and $\Delta\Psi$ in corn root membrane vesicles: Kinetic analysis of Cl^- effects on proton-translocating ATPase. J Membr Biol **71:** 95–107
2. **Briskin DP, Thornley WR, Wyse RE** (1985) Membrane transport in isolated vesicles from sugarbeet taproot. I. Isolation and characterization of energy-dependent H^+-transporting vesicles. Plant Physiol **78:** 865–870
3. **Chiu VCK, Mouring D, Watson BD, Haynes DH** (1980) Measurement of surface potential and surface charge densities of sarcoplasmic reticulum membranes. J Membr Biol **56:** 121–132
4. **Deleers M** (1985) Cationic atmosphere and cation competition binding at negatively charged membranes: pathological implications of aluminum. Res Commun Chem Pathol Pharmacol **49:** 277–294
5. **Dowd JE, Riggs DS** (1985) A comparison of estimates of Michaelis-Menton kinetic constants from various linear transformations. J Biol Chem **240:** 863–869
6. **DuPont FM** (1987) Variable effects of nitrate on ATP-dependent proton transport by barley root membranes. Plant Physiol **84:** 526–534
7. **Duzgunes N, Nir S, Wilschut J, Rentz J, Newton C, Portis A, Papahadjopoulos D** (1981) Calcium and magnesium induced fusion of mixed phosphatidyl serine/phosphatidyl choline vesicles. Effect of ion binding. J Membr Biol **59:** 115–125
8. **Eraso P, Cid A, Serrano R** (1987) Tight control of the amount of yeast plasma membrane ATPase during changes in growth conditions and gene dosage. FEBS Lett **224:** 193–197
7. **Giannini JL, Briskin DP** (1987) Proton transport in plasma membrane and tonoplast vesicles from red beet (*Beta vulgaris* L.) storage tissue. A comparative study of ion effects on ΔpH and $\Delta\Psi$. Plant Physiol **84:** 613–618
10. **Giannini JL, Gildensoph LH, Briskin DP** (1987) Selective production of sealed plasma membrane vesicles from red beet (*Beta vulgaris* L) storage tissue. Arch Biochem Biophys **254:** 621–630
11. **Gibrat R, Romieu C, Grigon C** (1983) A procedure for estimating the surface potential of charged or neutral membranes with 8-anilino-1-naphthalene-sulphonate probe. Biochim Biophys Acta **736:** 196–202
12. **Gibrat R, Grouzis JP, Rigaud J, Grignon C** (1985) Electrostatic characteristics of corn root plasmalemma: effect of Mg^{2+}-ATPase activity. Biochim Biophys Acta **816:** 349–357
13. **Grieve CM, Fujiyama H** (1987) The response of two rice cultivars to external Na/Ca ratio. Plant Soil **103:** 245–250
14. **Gronwald JW, Suhayda CG, Tal M, Shannon MC** (1990) Reduction in plasma membrane ATPase activity of tomato roots by salt stress. Plant Sci **66:** 145–153
15. **Gunn RB** (1980) Co- and counter-transport mechanisms in cell membranes. Annu Rev Physiol **42:** 249–259
16. **Honig BH, Hubbell WL, Flewelling RF** (1986) Electrostatic interactions in membranes and proteins. Annu Rev Biophys Biophys Chem **15:** 163–193

17. **Lakowicz J** (1983) Principles of fluorescence spectroscopy. Plenum Press, New York
18. **Leonard RT** (1984) Membrane associated ATPases and nutrient absorption by roots. *In*: PB Tinker, A Lauchli, eds, Advances in Plant Nutrition, Vol I. Praeger Scientific, New York, pp 209–240
19. **Maas EV, Grieve CM** (1987) Sodium-induced calcium deficiency in salt-stressed corn. Plant Cell Environ **10:** 559–564
20. **McLaughlin S** (1977) Electrostatic potentials at membrane-solution interfaces. Curr Topics Membr Trans **9:** 71–143
21. **Nagahashi J, Nagahashi SL** (1982) Triton-stimulated nucleotide diphosphatase: characterization. Protoplasma **112:** 174–180
22. **Peterson GL** (1977) A simplification of the protein assay method of Lowry et al. which is more generally applicable. Anal Biochem **83:** 346–356
23. **Peterson GL** (1978) A simplified method for analysis of inorganic phosphate in the presence of interfering substances. Anal Biochem **84:** 164–172
24. **Poole RJ, Briskin DP, Kratky Z, Johnstone RM** (1984) Density gradient localization of plasma membrane and tonoplast from storage tissue of growing and dormant red beet: characterization of transport and ATPase in tonoplast vesicles. Plant Physiol **74:** 549–556
25. **Suhayda CG, Weis C, Shi B, Haug A** (1988) pH-related changes in maize root plasma membranes. Commun Soil Sci Plant Anal **19:** 1165–1175
26. **Sze H** (1985) H^+-translocating ATPases: advances using membrane vesicles. Annu Rev Plant Physiol **36:** 175–208